

Single Cell Profiling of Potentiated Phospho-Protein Networks in Cancer Cells

Jonathan M. Irish,¹ Randi Hovland,^{2,3}
Peter O. Krutzik,¹ Omar D. Perez,¹
Øystein Bruserud,^{3,4} Bjørn T. Gjertsen,^{3,4}
and Garry P. Nolan^{1,*}

¹Department of Microbiology & Immunology
Baxter Laboratory of Genetic Pharmacology
Stanford University
Stanford, California 94305

²Center for Medical Genetics and Molecular
Medicine
Haukeland University Hospital and Proteomic Unit
(PROBE)
University of Bergen
Bergen
Norway

³Department of Internal Medicine
Haematology Section
Haukeland University Hospital
Bergen
Norway

⁴Institute of Medicine
Haematology Section
University of Bergen
Bergen
Norway

Summary

Altered growth factor responses in phospho-protein-driven signaling networks are crucial to cancer cell survival and pathology. Profiles of cancer cell signaling networks might therefore identify mechanisms by which such cells interpret environmental cues for continued growth. Using multiparameter flow cytometry, we monitored phospho-protein responses to environmental cues in acute myeloid leukemia at the single cell level. By exposing cancer cell signaling networks to potentiating inputs, rather than relying upon the basal levels of protein phosphorylation alone, we could discern unique cancer network profiles that correlated with genetics and disease outcome. Strikingly, individual cancers manifested multiple cell subsets with unique network profiles, reflecting cancer heterogeneity at the level of signaling response. The results revealed a dramatic remodeling of signaling networks in cancer cells. Thus, single cell measurements of phospho-protein responses reveal shifts in signaling potential of a phospho-protein network, allowing for categorizing of cell network phenotypes by multidimensional molecular profiles of signaling.

Introduction

Intracellular signaling and interpretation of environmental cues play central roles in cancer cell initiation and maintenance. Actions that lead to cancer cell progres-

sion include mutations to key signaling proteins as well as epigenetic changes to gene expression patterns (Hanahan and Weinberg, 2000). Cancer genesis occurs in a stepwise progression, has underlying stochastic elements, and is reflective of the genetic selection of the cancer in the face of both immune system action and the environmental requirements of cancer cells. The signaling profile of any given cancer cell is therefore the sum of numerous influences: epigenetic, genetic, and microenvironmental. The current molecular understanding of cancer signaling rests largely on extrapolations from studies of cell lines and as such is not adequately representative of the signaling phenotypes of a complex population of cancer cells in the body. In contrast, the heterogeneity of cancer cell responses to therapy can be thought of as mirroring the signaling differences that have arisen during evolution of the cancer cell population in the body. Until now, this cell by cell information on cancer cell populations—required to model signaling network pathologies that relate to cancer cell subsets and disease progression—has not been available for analysis.

Phospho-protein members of signaling cascades, and the kinases and phosphatases that interact with them, are required to initiate and regulate proliferative signals within cells. It might be predicted that genetic changes common in cancers, such as receptor tyrosine kinase mutations and other signaling-related cytogenetic alterations (Spiekermann et al., 2002; Wheatley et al., 1999), would change the potential of pre-existing signaling networks to respond to external stimuli and lead to identifiable patterns of signal transduction associated with gene mutation. For instance, acute myeloid leukemia (AML) is a cancer wherein dysregulated growth and inhibition of apoptosis lead to the accumulation of immature myeloid progenitor cells and oncogenic progression (Lowenberg et al., 1999). Two key parallel signal transduction networks active in cells that are considered progenitors of AML (Reya et al., 2001) are the STAT pathway (Coffer et al., 2000; Smithgall et al., 2000) and the Ras/MAPK pathway (Platanias, 2003). Several reports suggest that STATs, such as Stat3 and Stat5, are constitutively activated in AML (Benekli et al., 2002; Birkenkamp et al., 2001; Turkson and Jove, 2000; Xia et al., 1998). But, a causal link between basal STAT phosphorylation and leukemogenesis in primary patient material has not been demonstrated, despite significant evidence implicating these proteins in oncogenic processes (Benekli et al., 2003; Bowman et al., 2000; Buetner et al., 2002; Calo et al., 2003; Nieborowska-Skorska et al., 1999). Thought to act upstream of these pathways, abnormalities of the Flt3 (*fms*-like tyrosine kinase 3) receptor tyrosine kinase are detected in approximately 30% of AML patients and are well established as a negative prognostic indicator in AML (Gilliland and Griffin, 2002; Kottaridis et al., 2001; Thiede et al., 2002). Expression of mutant, activated Flt3 in cell lines has been observed to activate STAT and Ras/MAPK signaling (Hayakawa et al., 2000; Mizuki et al., 2000). However, basal levels of Stat5 phosphorylation have been reported to

*Correspondence: gnolan@stanford.edu

be statistically indistinguishable in Flt3 mutant and wild-type patient-derived AML blasts (Pallis et al., 2003). The differences observed between cell line studies and primary patient samples raises the question of why, in primary cells, there is not a strong linkage between activating mutations in signaling proteins, increased basal phosphorylation of putative targets, and disease state.

Upon consideration, it could be proposed that it is not the absolute level of the signaling proteins themselves (or their basal phosphorylation status) that will be most informative of cancer signaling processes, but the manner in which such proteins perform in signaling networks. A potentially informative approach to illuminate the structure of signaling networks would be to impose a signaling input on cancer cells and monitor changes in the level of phosphorylation on multiple key nodal proteins. As such, one could measure the effects of known (and unknown) mutations on signaling events in cancer cell subtypes. Furthermore, one could detect the influence of such mutations in sensitizing or potentiating the response of the cancer cell to other inputs or environmental cues. By providing multiple discrete inputs to the signaling system, one is theoretically polarizing signaling networks to reveal their underlying structure(s). Thus, by simultaneously measuring multiple phosphorylation events at the single cell level across a complex population of cancer cells, it would be possible to build and distinguish pathway anomalies in different cell subsets. This could allow for resolution, in different individuals, of those signaling profiles that differentiate cancer subtypes and relate to disease progression. We describe this as interrogating the potentiation of signaling pathways—that is, stimulating a network to reveal its signaling potential.

A cohort of adult AML patients with characterized mutations in Flt3 and known cytogenetic abnormalities (Bruserud et al., 2003) provided us with an opportunity to compare gene mutations with signal transduction profiles in primary cancer samples. To meet a standard of measuring signaling events simultaneously in a controlled context we used intracellular phospho-specific flow cytometry (Krutzik and Nolan, 2003; Perez and Nolan, 2002) to detect multiple phosphorylated, activated signaling molecules in primary leukemic cells drawn from this cohort of well-characterized AML patients. Flow cytometry is useful in a clinical setting as relatively small sample sizes—as few as 10,000 cells collected—can produce a considerable amount of statistically tractable multidimensional signaling data and reveal key cell subsets responsible for a phenotype (Krutzik et al., 2004). We tested the hypothesis that genetic alterations to signaling genes would cause leukemic cells to react in an inappropriate or sensitized manner to environmental inputs and that this differential signaling can be read out by single cell flow cytometry.

Here, we apply potentiated signaling to interrogate multiple key nodal phospho-proteins in cancer networks, map signaling mechanisms that unite cancer subtypes, and demonstrate an intimate association between oncogene mutation, remodeling of signaling networks, and pathology. The profiles of signal transduction that correlated with poor response to chemotherapy showed potentiated Stat5 and Stat3 phosphorylations

as well as attenuated Stat1 phosphorylation following cytokine stimulation. This is consistent with a model where AML arises from proliferative signaling in the absence of differentiation and apoptosis. Therefore, potentiated signaling can reveal relationships in phospho-protein networks that are reflective—either causal or reactive—of the mutations thought to initiate or sustain the growth of a particular cancer phenotype and might be applicable to mapping of signaling changes during normal development.

Results

Phospho-Protein Response Panel Distinguishes Leukemic Signal Transduction Networks

A cytokine response panel, composed of 36 phospho-protein states (6 basal states and 30 cytokine responses), was designed to survey altered signal transduction of cancer cells (Figure 1A). Each square in the grid approximates a multidimensional flow cytometry file that contained at least 30,000 cell events. The cytokine responses of each phospho-protein node were compared to the basal state (shown in this profile set as normalized to black) and represented by calculating the \log_2 fold difference in median fluorescence intensity (MFI) of stimulated sample divided by unstimulated sample. Although the data are visually simplified in a response panel, the multiparameter flow cytometry data are available for further inspection of single cell phospho-protein responses of interesting subsets, as examined in detail later (Figure 5).

The cytokine response panel included detection of phosphorylated Stat1, Stat3, Stat5, Stat6, p38, and Erk1/2. We collected data on unstimulated cells and cells stimulated for 15 min with Flt3 ligand (FL), GM-CSF, G-CSF, IL-3, or IFN γ . This panel was applied to the U937 histiocytic lymphoma cell line (Figure 1A), the HL-60 AML cell line, and multiple samples of a CD33⁺ subset from normal peripheral blood (Figure 1B). CD33⁺ cells represent differentiated cells of myeloid lineage and were used to assess variability in cytokine responses among samples from blood donors. In general, the cytokine responses of normal lymphocyte subsets differed very little between normal donors ($\sigma^2 < 0.1$, $n = 6$).

In contrast, the cytokine responses of AML cells varied in numerous ways between patient samples. The cytokine response panels for 6/30 representative AML patient samples are shown (Figure 1C, AML-P01 through -P06). For example, although AML-P02 and AML-P03 displayed many similarities, AML-P02 responded to GM-CSF and G-CSF with phosphorylation of Stat5 while AML-P03 responded only to GM-CSF at Stat5 (Figure 1B). Additionally, although most patient samples and controls displayed potent phosphorylation of Stat1 following IFN γ , AML-P05 lacked this response. Repeat measurements of cell lines, primary cell samples, and AML samples were collected ($n \geq 3$) and the technique and monoclonal antibodies displayed a high level of reproducibility similar to previous studies (Krutzik and Nolan, 2003).

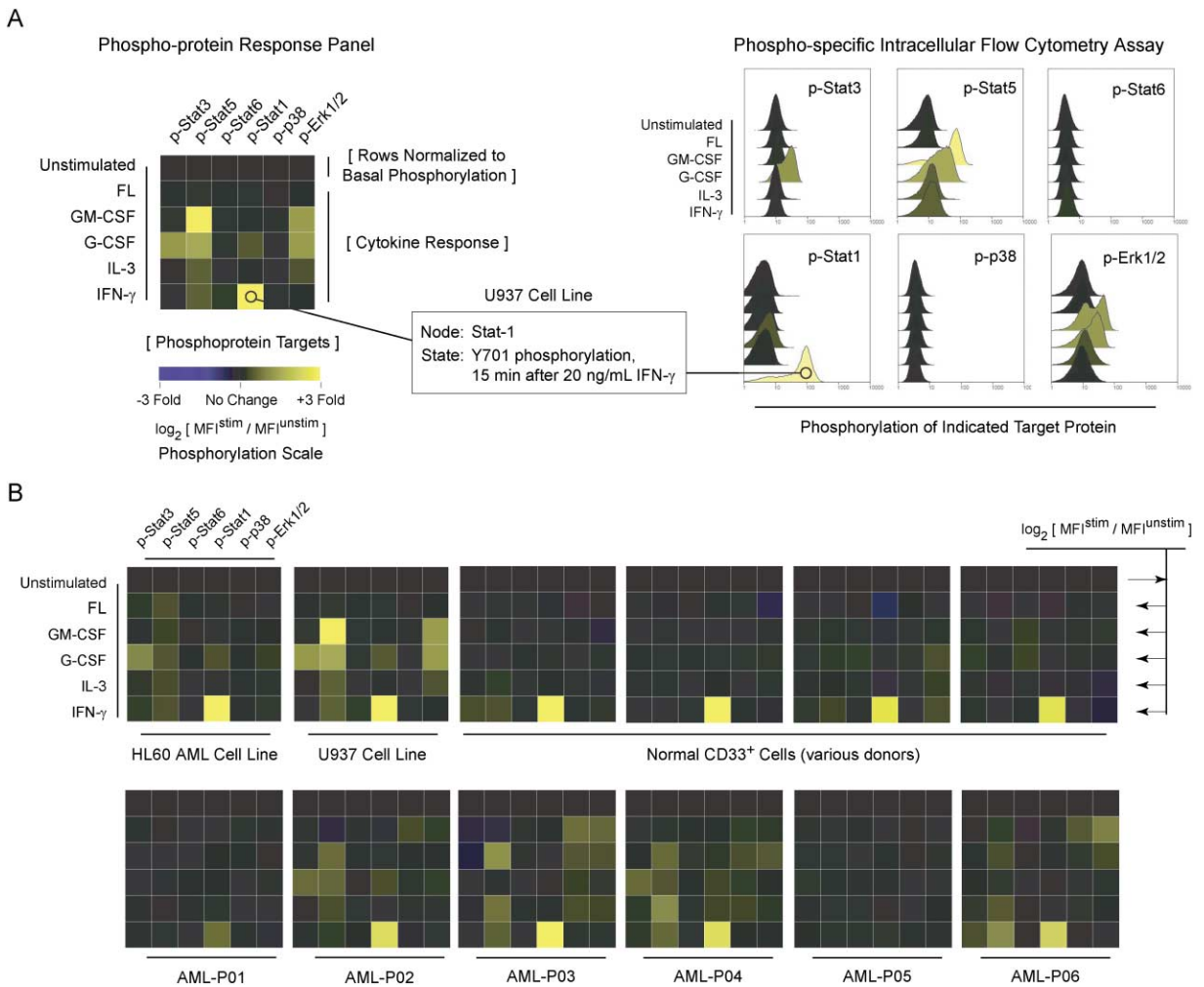


Figure 1. A Cytokine Response Panel Reveals Potentiated Signal Transduction Nodes in Primary Acute Myeloid Leukemias

(A) Stimulation states, shown in rows, included unstimulated or 20 ng/ml of FL, GM-CSF, G-CSF, IL-3, or IFN γ . Target phosphorylations were detected using phospho-specific antibodies for Stat1, Stat3, Stat5, Stat6, p38, and Erk1/2, shown in columns. Each square in the grid represents the response of one phosphorylation site to one condition. The relationship between the grid and the flow cytometry data on which it is based is diagrammed for U937 cells.

(B) Representative cytokine response panels of the HL-60 AML cell line, normal CD33⁺ leukocytes, and six AML patient samples. Repeat experiments using these AML blasts yielded similar results ($n = 3$), and variation among normal, healthy donors was minimal ($n = 6$). The response to stimulation at each signaling node is calculated as $\log_2 (MFI^{stimulated}/MFI^{unstimulated})$.

Basal Phosphorylation and Cytokine Responses of STAT and Ras-MAPK Phospho-Proteins Vary Significantly among Primary AML Patient Samples

Phospho-protein responses in many of the primary AML blasts showed considerable induction and variance of STAT and RAS/MAP-K pathway member phosphorylation (Figure 2A). To illustrate the differences in the basal state across the AML samples, the first row of each basal state has been represented according to a heat map relative to the minimum among the 30 AML patient blasts tested. As can be seen, there is considerable variation across all basal nodes. However, some signaling nodes remain activatable, and, following stimulation, we observed phosphorylation of associated signaling proteins above the level observed in the basal state. In addition to the considerable variation of the six basal

phosphorylation states, we identified 7 of the 30 cytokine response states that displayed significant variance across AML patient samples ($\sigma^2 > 0.1$, Figure 2B). These were (1) phosphorylation of Stat3 following G-CSF, (2–5) phosphorylation of Stat5 following GM-CSF, G-CSF, IL-3, and IFN γ , (6) Stat1 phosphorylation following IFN γ , and (7) phosphorylation of Erk1/2 following FL. The remaining cancer cytokine responses displayed variation at or less than the variance in normal, differentiated CD33⁺ cells (Figure 1B). Including the two closest node states to the significance threshold did not affect subsequent patient groupings (Supplemental Figure S1 at <http://www.cell.com/cgi/content/full/118/2/217/DC1>). Removing further nodes did affect the clustering, suggesting that this collection of nodes represents the minimum set of node states from this analysis for an accurate

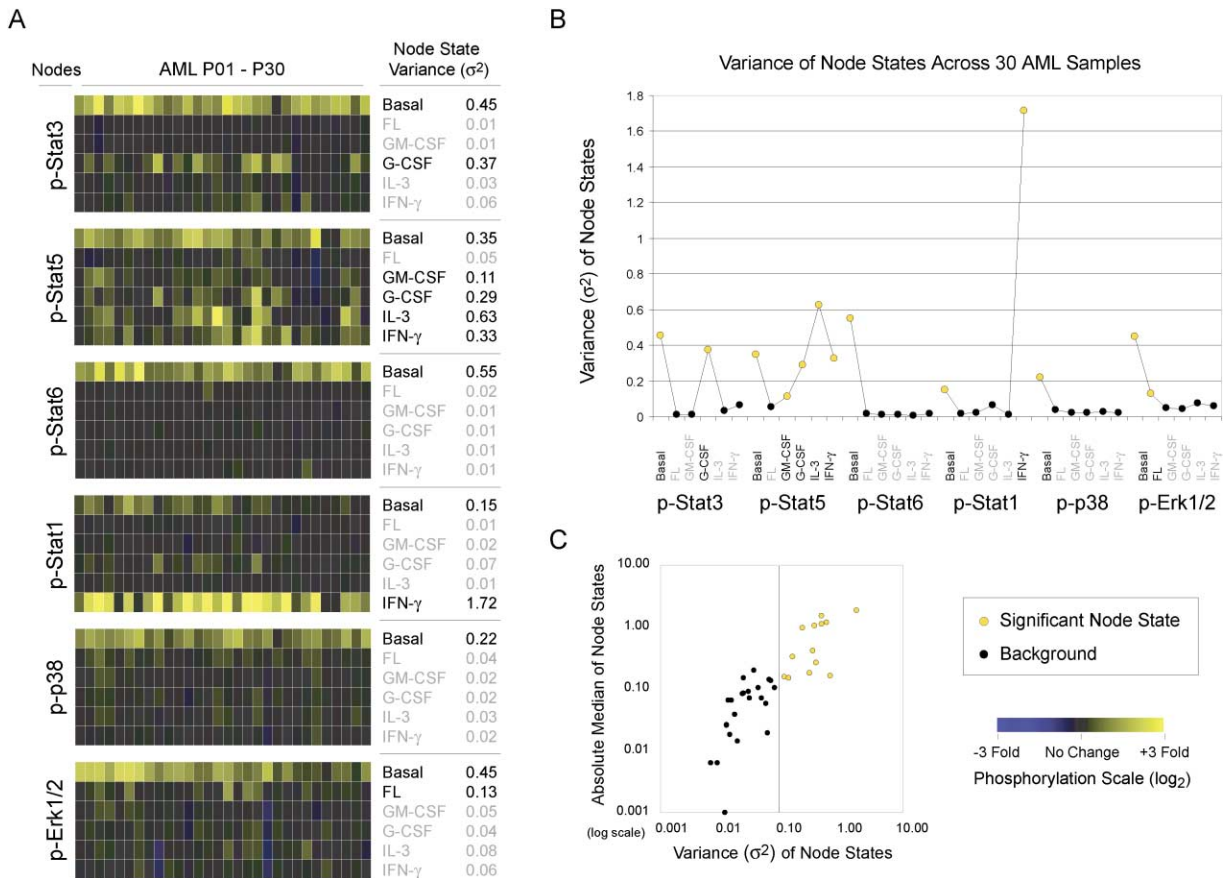


Figure 2. Basal and Potentiated Signaling Nodes that Varied among Cancer Samples Were Used to Define an AML Biosignature
 (A) The cytokine response panel of 30 total AML patient samples. The first row of each has been colored to show the variation in the basal phosphorylation (relative to the minimum among the AML blasts). Of 900 cytokine responses assayed, 93 (10.3%) displayed a detectable phosphorylation increase following stimulation (greater than 0.55-fold on a \log_2 scale).
 (B) Significant cytokine responses were restricted primarily to the 7/30 cytokine response nodes with a variance across cancers greater than 0.1 (yellow circles).
 (C) A graph of the absolute median plotted against the variance for each node state indicates the signal-to-noise threshold.

signaling profile. A graph of the absolute median against the variance indicates the signal-to-noise threshold and the relationship of variance to the median basal state or cytokine response (Figure 2C).

AML Patients with Similar Signal Transduction Profiles Display Similar Chemotherapy Responses, *Fli3* Mutations, and Cytogenetic Alterations

We composed a signal transduction based classification for AML using unsupervised clustering of phospho-protein biosignatures (Figure 3A). This was a first step in determining whether underlying networks showed mechanistic similarities to each other that corresponded with responsiveness to apoptotic induction by chemotherapy. Samples were grouped using the complete linkage hierarchical clustering algorithm available in Multiple Experiment Viewer (MeV) (<http://www.tigr.org/software/tm4/mev.html>). There are several advantages to unsupervised clustering based on potentiated signaling. When patients are clustered according to a biological hypothesis and then subsequently tested for correlation to clinical

parameters—as opposed to pre-grouping patients by clinical outcome and then testing each node state as a hypotheses—the statistical perils of multiple t tests can be minimized or avoided (Tilstone, 2003). This method also allows for disease subgroups to be identified even when normal control cells are rare or difficult to obtain in bulk, as is the case with myeloid progenitor cells (Reya et al., 2001), because differences among experimental samples are used to define groups rather than comparison of each sample to a proposed normal control.

Unsupervised clustering identified four main groups of AML patients (Figure 3A). Each of these groups was termed a signaling cluster (SC) and was referred to based on the primary signaling profile of the cluster: (1) SC-nonpotentiated (NP) had varied basal phosphorylation but displayed little or no potentiated phosphorylation in response to cytokine induction and a low Stat1 response to IFN γ (italic letters denote the cognate acronym), (2) SC-potentiated-basal (PB) displayed both a potentiated phosphorylation response to cytokine and high basal phospho-protein states, (3) SC-potentiated-1 (P1) displayed intense potentiated signaling, lower basal

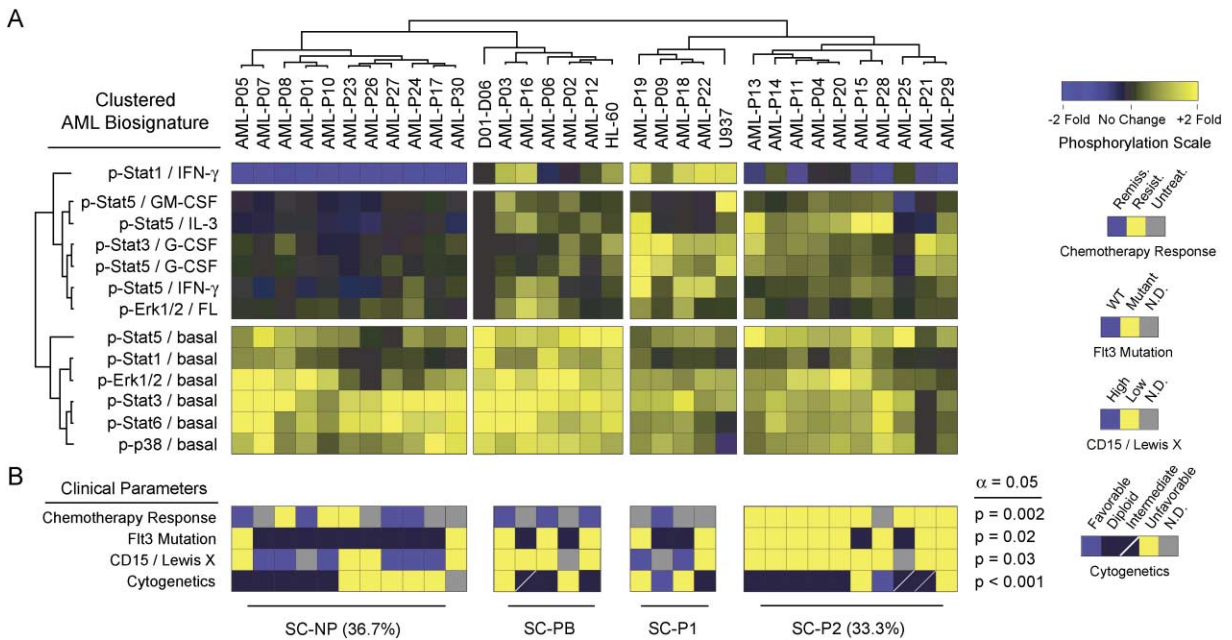


Figure 3. AML Patients Grouped by Signal Transduction Biosignature Form Four Groups that Exhibit Significant Correlations to Clinical Prognostic Markers

(A) The 13-parameter biosignatures of differentiated CD33⁺ myeloid cells from six normal blood donors (D01 – D06), U937 and HL-60 cancer cell lines, and 30 AML patient samples were grouped according to similarity using hierarchical clustering. The heat map for AML and cancer cell line cytokine responses was scaled by subtracting donor sample medians to provide a dynamic color range. As shown previously, basal responses are relative to the minimum among AML samples.

(B) Four main groups of AML patients were identified based on the similarity of their signal transduction biosignatures. We designated these groups with signaling cluster (SC) nomenclature based on the signaling that defined them and mapped several clinical markers within the identified patient groups.

phosphorylation, and a p-Stat1 response to IFN γ , and (4) SC-potentiated-2 (P2) displayed many potentiated cytokine responses in the context of low basal phosphorylation and a low Stat1 response to IFN γ .

Several clinical parameters were nonrandomly distributed among the SCs, and four of these are aligned below the heat map (Figure 3B). A full chart of known AML patient characteristics, ordered by SC, is provided for further analysis (Supplemental Table S1 on the *Cell* website). The χ^2 statistical test was used to determine the significance of the observed correlations between clinical factors previously determined to be prognostic for AML and the biosignature-derived SCs.

Resistance to course one chemotherapy correlated significantly with clustered signaling groups and occurred primarily in patients with an SC-P2 profile ($p = 0.002$, Figure 3B). Patients with an SC-P2 profile constituted 33% of this cohort (10/30) and were primarily defined by potentiated Stat5 and Stat3 myeloid signaling in the absence of Stat1 phosphorylation following IFN γ . AML patient samples that displayed high myeloid cytokine responses usually contained an internal tandem duplication of FIt3—whereas the samples with a nonpotentiated SC profile lacked these mutations ($p = 0.02$). In testing the correlation of six cell surface antigens with SC groups or FIt3, we noted that low expression of CD15/Lewis X significantly correlated with SC-P2 and FIt3 mutation ($p = 0.03$ and $p < 0.001$, respectively, Figure 3B).

In patients with an SC-NP profile, cytogenetic alter-

ations were grouped into a closely related branch (Figure 3, hierarchy branch AML-P23 through AML-P30) containing two patients with a 9;11 translocation (AML-P27 and AML-P24) and two patients with a loss of chromosome 5 (AML-P23 and AML-P17). Patients with no detected cytogenetic alterations formed a closely related branch of SC-P2 (Figure 3A, hierarchy branch AML-P13 through AML-P20). This division of altered or diploid cytogenetics among branches of SC-NP and SC-P2 was statistically significant ($p < 0.001$).

The signaling profiles and the activities represented can be viewed in a more conventional network map (see Figure 6) in an attempt to relate mechanism to signaling outcome. With the SC-P2 cluster, a composite pathway shows the action of multiple basal state activators (in orange) that induce a “basal high” status for the targeted phospho-proteins (for SC-P2, only p-Stat5). In addition, this map shows that one or more of several upstream activators can induce higher levels of phosphorylation above the basal phosphorylation level (representing that these nodes are activatable). In contrast, with SC-NP profiles, high basal phosphorylation at signaling nodes was observed (p-Erk1/2, p-Stat3, and p-Stat6), but additional phosphorylation was not usually observed following stimulation. These pathway maps are based on observations of signaling by flow cytometry (Figure 5) and are built to represent signaling clusters (Figure 3). Thus, while individual AML samples showed differences from the composite representations (Figure 7 and see Discussion), signaling profile correlations can be clearly identi-

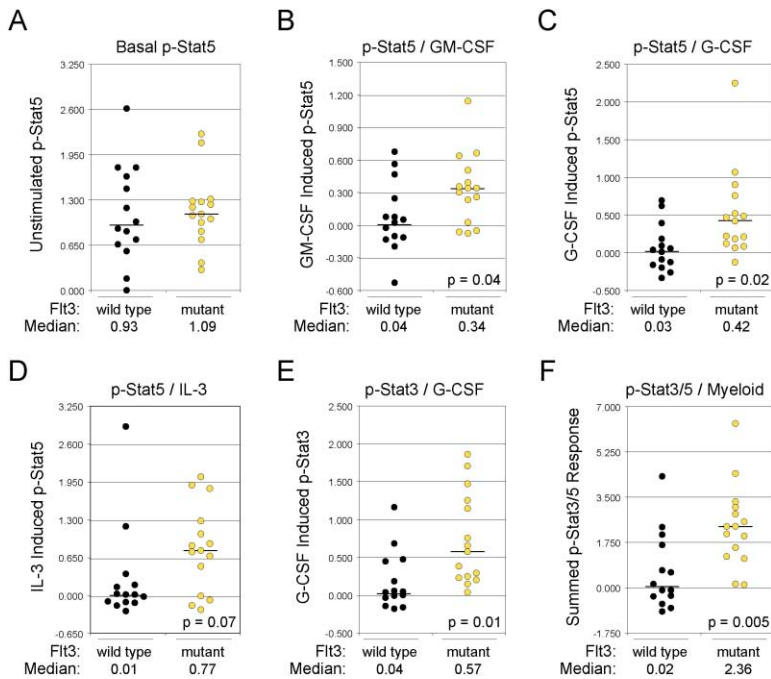


Figure 4. Flt3 Mutation in Primary AMLs Is Associated with Potentiated Myeloid Signal Transduction Nodes

Basal and cytokine response node states of patient samples with wild-type or mutant Flt3 are shown for the 30 AML samples assayed. Each circle represents the level of STAT phosphorylation detected in an individual AML patient sample, grouped according to wild-type Flt3 (black) or detected mutant Flt3 (yellow). (A) To assess basal phosphorylation, samples were compared to the minimum observed among cancers. (B–E) The phosphorylation of Stat5 detected following GM-CSF, G-CSF, and IL-3 and of Stat3 following G-CSF is shown as a fold increase above basal. (F) Cumulative myeloid cytokine responses, calculated by summing individual responses (B–E), were compared in patients with and without Flt3 mutations.

fied for groups (Figure 6), related to mechanisms, and used to form new hypotheses.

AML Blast Cells from Patients with Flt3 Mutations Display Increased Stat5 and Stat3 Phosphorylation in Response to GM-CSF and G-CSF

We used a t test to assess the significance of the observed correlation between Flt3 mutation and potentiated myeloid signal transduction. The cytokine responses of patient samples with Flt3 mutations were compared with patient samples that had no detectable receptor tyrosine kinase mutation (Figure 4). We observed no significant difference in the basal phosphorylation of Stat5 in either normal or Flt3 mutant AML samples (Figure 4A), as had been previously observed in patient samples (Pallis et al., 2003). Because expression of mutant Flt3 had been demonstrated to have a potent effect on Stat5 phosphorylation in cell lines, we asked whether there was a connection between Flt3 mutations and potentiated Stat5 and Stat3 phospho-protein signaling.

Four of the p-Stat5 and p-Stat3 myeloid cytokine responses were identified as displaying significant variance across cancers (Figure 2; p-Stat3 following G-CSF, and p-Stat5 following GM-CSF, G-CSF, and IL-3), so we compared these responses in samples with and without Flt3 mutation. Phosphorylation of Stat5 following GM-CSF and G-CSF was significantly potentiated in patient samples with Flt3 mutations ($p = 0.04$ and 0.02 , respectively; Figures 4B and 4C). Sample calculations of t values are provided (Supplemental Table S2 online). Phosphorylation of Stat5 following IL-3 correlated with Flt3 status, but this was not statistically significant ($p = 0.07$, Figure 4D). Stat3 phosphorylation following G-CSF, the only Stat3 biosignature response state displaying significant variance among AMLs, correlated significantly with

Flt3 mutation ($p = 0.01$, Figure 4E). Other cytokine responses were not observed to differ in patients with and without Flt3 mutation. To represent a combined effect of Flt3 mutation on myeloid signal transduction nodes, we summed these four cytokine response node states. This correlation between myeloid cytokine responses and Flt3 mutation in AML patient samples was significant ($p = 0.005$), and all samples with detectable Flt3 mutations displayed positive myeloid cytokine responses (Figure 4F). Thus, there is a strong linkage between the responsiveness of the cells to this set of myeloid stimuli and oncogenic mutation of Flt3, suggesting that activating mutations of Flt3 potentiate certain elements of the AML response beyond those which are canonically observed.

Multidimensional Single Cell Profiling Reveals Cancer Cell Subsets with Distinct Signal Transduction Profiles

Flow cytometry has the ability to simultaneously measure multiple events per cell and, as such, has allowed the delineation of phenotypic distinctions of immune and other cell subsets. We aimed to determine whether data simultaneously collected on two phospho-protein states (Krutzik et al., 2004) in these AML samples showed signaling differences that suggested cancers were composed of different subsets of cells with distinct signaling modes. Two-dimensional contour plots for the G-CSF response of Stat5 and Stat3 are shown (Figure 5) grouped according to the signaling cluster hierarchy (which is correlated with the Flt3 mutational status)—for cognate AML patient samples (see Supplemental Figure S2 for a complete two-dimensional flow cytometry dataset). G-CSF stimulated both Stat3 and Stat5 phosphorylation and, to a large extent, this dual signaling took place simultaneously in individual cells. The linked potentiation of p-Stat5/G-CSF and p-Stat3/G-CSF in indi-

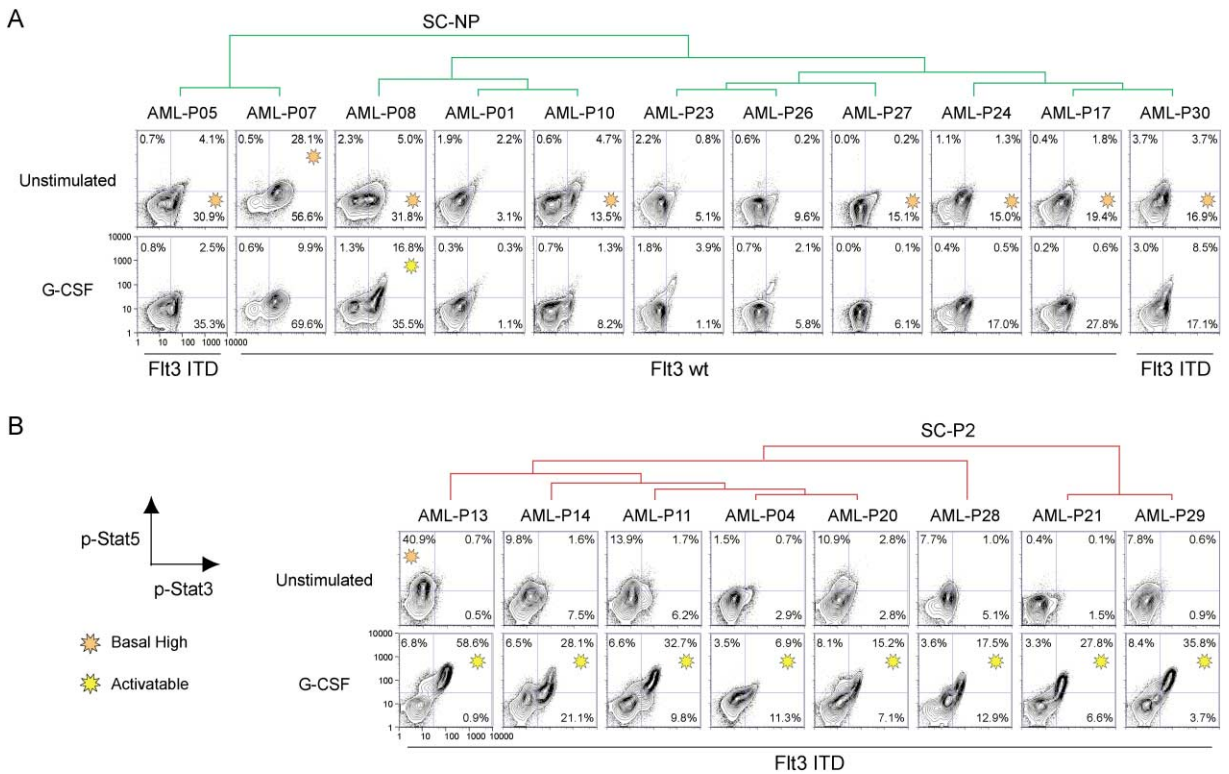


Figure 5. Representative 2D Flow Cytometry Plots of Stat5 and Stat3 Phosphorylation following G-CSF Stimulation in AML Patient Samples with Wild-Type FIt3 and Mutant FIt3 (ITD)

Two-dimensional contour plot representations of Stat5 and Stat3 phosphorylation (y and x axis, respectively) in patient samples from SC-NP and SC-P2. Both the level of basal phosphorylation and the response to G-CSF are shown.

vidual primary AML blast cells was most common in samples with detectable FIt3 mutations (Figure 5B). However, we noted the reproducible presence of single positive subpopulations in some patients (note AML-P13 and P20 as compared to P11). Thus, significant cancer heterogeneity at the level of signaling heterogeneity can be observed.

Four of the SC-NP profiles revealed the presence of a small, induced, p-Stat5/p-Stat3 double-positive subpopulation (AML-P08, P23, P26, P30, Figure 5A). This raises the interesting possibility that the presence of a double positive, G-CSF-inducible p-Stat5/p-Stat3 subpopulation, independent of obvious FIt3 mutational status, is predictive of an aggressive form of AML that is not subject to DNA damage induction of apoptosis. In some of these patients with a double positive p-Stat5/p-Stat3 response to G-CSF, we did not observe FIt3 mutation, though it is possible that additional mutations in other regulators phenocopy the effect of the FIt3 mutation. Of chemotherapy-treated patients with detectable FIt3-ITD mutation and a non-SC-P2 profile (4 treated, 3 were too sick to be treated), 4/4 went into remission following course 1 chemotherapy. In contrast, 7/7 patients with an SC-P2 profile and FIt3-ITD mutation relapsed following chemotherapy. In this cohort, detection of an SC-P2-potentiated signaling profile provided a better prediction of chemotherapy response than that obtained through identification of FIt3 mutation alone. Therefore, the signaling profile of samples with detect-

able mutations may indicate whether these mutations successfully elicit potentiated signaling, which these data suggest would be predictive of aggressive pathology. Higher dimensional resolution with additional stimuli, or groups of stimuli, and downstream phospho-readouts could provide the additional data that would provide a mechanistic insight to answer this question, as discussed below.

Discussion

We observe that the varied genetic and clinical phenotypes of leukemic cancers are profoundly linked to discernible patterns in phospho-protein signal transduction networks. This allowed us to map signal transduction mechanisms of cell subsets within individual patient samples, cluster patient samples based on signaling profiles, and ultimately observe that certain leukemic signaling profiles of phospho-protein targets were significantly linked with mutation of FIt3, cytogenetic changes, expression of the cell surface marker CD15, and response to chemotherapy. Critical to successful clustering was the inclusion of the response of signaling networks to environmental cues, along with the basal levels of phosphorylation. Such profiling can be used to (1) understand signaling mechanisms in malignant progression, (2) describe cancers by molecular phenotype, and (3) translate this information for clinical applications. Thus, the signaling phenotype associated with

a particular cell context (differentiation state, activation or proliferation capacity, mutation, or class of mutations) can be revealed in the pattern of phosphorylations detected when that network is queried to process stimuli.

Potentiated Signaling Reflects Underlying Network Differences

For many years, researchers have attempted to link activities of protein(s) to phenotypic outcomes in cancer progression and response to chemotherapy. We observed that by stimulating networks of phosphoproteins in leukemic cells to respond to environmental cues, we “align” these proteins according to the network’s response potential. Thus, in AML cancers with varying pathology and disease origin, responses to environmental cues grouped AML types according to the underlying performance boundaries of their signal transduction networks (whose response is driven in part by the mutations that occurred during the history of that cancer). As an example, although AML-P14 and AML-P24 had relatively similar patterns of basal STAT and Ras-MAPK pathway phosphorylation, these samples exhibited very different phospho-protein patterns following cytokine stimulation (Figure 3A) and had differences in chemotherapy response, *Fit3* mutational status, and cytogenetics (Figure 3B and Supplemental Table S1 online). So while a profile of basal signaling alone would have found these two patient samples to be similar, by using the response to environmental cues combined with a clustering analysis to group similar molecular phenotypes, we identified key differences in the signaling networks of the cancer cells in these two samples.

Each response node in the cluster can be mapped to a potential for a phospho-protein to be activated by an upstream signaling event. Or, the node can be mapped as a basal state that is activated above background levels (shown in orange as an auxiliary input to the signaling system, Figures 6 and 7). Thus, we see there are significant differences in signaling mechanisms defining composite groupings of SC-P2 and SC-NP (Figure 6). The composite SC-P2 profile (which is characterized primarily by response to cytokine stimulation above basal levels) had high basal Stat5 and lower basal phosphorylation at other nodes and could be potentiated for Stat5, Stat3, or Erk by one of many cytokines. In strong contrast, SC-NP was nonresponsive to upstream stimuli but had varying basal high levels of Stat3, Stat6, and Erk and was low basal for Stat5. Thus, the primary distinction between the two groups was that one group had low basal phosphorylation levels but responded to environmental cues, while the second group had high internal basal phosphorylations at some of these phosphoprotein nodes, but these nodes were nonresponsive to upstream environmental inputs such as cytokine stimulation.

Under this hypothesis of potentiated signaling, we predicted that particular signal transduction profiles, such as niche-specific, pro-survival patterns, would correlate with resistance to chemotherapy-induced cell death. We observed that the response to course one of chemotherapy was a relapse in 9/9 treated patients whose samples displayed an SC-P2 profile (Figure 3), a pattern characterized by multiple potentiated myeloid

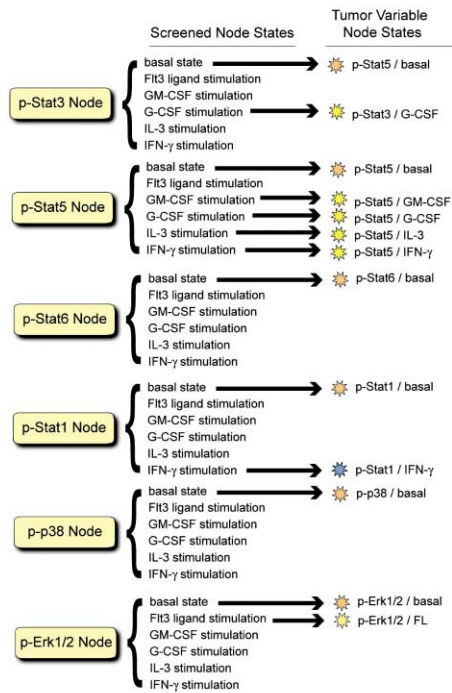
signaling states (p-Stat5, p-Stat3, p-Erk1/2) found in combination with a low p-Stat1/IFN γ response and high basal Stat5 phosphorylation (Figure 3). This demonstrates that signal transduction-based classification of human cancer, a priori of knowledge of clinical outcome, can produce a patient classification that is predictive of response to therapy.

Although a common SC-P2 profile emerged, at the individual sample level we observed differences in signaling mechanisms contributing to STAT and Ras-MAPK potentiation (Figures 7A–7C). For example, AML-P11, AML-P21, and AML-P29 were all profiled as SC-P2, had detectable *Fit3* mutations, and relapsed following chemotherapy. In looking at their individual signaling profiles, we see that AML-P11 had high basal Stat5 phosphorylation in resting cells but also was able to phosphorylate Stat5 following G-CSF, IL-3, and IFN γ . Cells from AML-P21 displayed responses in p-Stat5 to G-CSF and IFN γ but lacked high resting phosphorylation of Erk1/2 and Stat5. In AML-P29, we detected low basal phosphorylation but observed that Stat5 was phosphorylated following numerous stimuli. While Stat5 provided a common link in these signaling systems in that it was capable of being activated above basal levels, variations existed in other nodes (see Figure 7 for details). What united this group was that cancers exhibiting a lack of response to chemotherapy (a DNA damage-inducing regimen that induces cell death via apoptosis) were composed of cell subsets with common potential to respond to one or more upstream cytokine activators and could frequently be detected to have an activating mutation in a signaling gene (e.g., *Fit3*-ITD). In common between SC-P2 and SC-NP was that both profiles portray at least one upregulated basal state that likely contributes to driving cellular division, but the ability to activate further signaling past basal levels was what enabled correlation of signaling profiles with a lack of response to chemotherapy.

In the signaling cluster groups, basal phosphorylation differences helped distinguish between subgroups with cytogenetic alterations (branches of SC-NP and SC-P2, Figure 3). Patient samples with cytogenetic alterations were distinguished from samples with diploid cytogenetics in branches of the two main SCs ($p < 0.001$, Figure 3). This suggests that the signal transduction profile of leukemic blasts reflects the presence or absence of karyotypic abnormalities and that cytogenetic changes at different loci can lead to similar effects (phenocopying) on the signal transduction profile of a cell. In addition, correlation of *Fit3* mutation with low CD15/Lewis X antigen expression ($p < 0.001$, Figure 3) had not previously been reported. A connection between *Fit3* signaling and CD15 expression has been observed in models of myeloid cell expansion where FL injection following transplantation of bone marrow cells to a SCID-hu mouse resulted in increased relative numbers of CD33 $^+$ /CD15 $^-$ cells (Namikawa et al., 1999).

As reported by others (Pallis et al., 2003), we observed no significant difference in basal phosphorylation of Stat5 between normal and *Fit3* mutant AML patients (Figure 5). The results suggest that the presence of *Fit3*-ITD is linked with potentiation or sensitization of the phosphorylation of Stat5, and possibly Stat3, in response to the myeloid cytokines GM-CSF and G-CSF

A



Phospho-protein Biosignature of AML

B

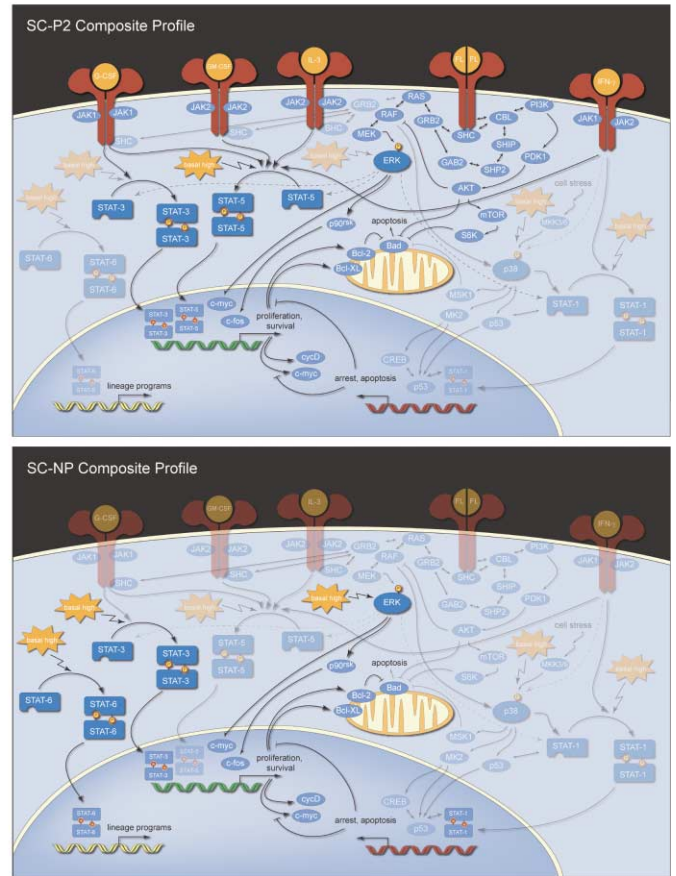


Figure 6. Cancer Biosignatures and a Potentiated Model of Cancer Cell Signaling

(A) A general method for identifying a cancer biosignature is shown using an example of STAT and Ras/MAPK signaling node states in AML. (B) Composite maps of cancer networks from profiles SC-NP and SC-P2 were built out of common signaling events observed in each cluster. Highlighted nodes were detected to be high basal or potentiated in most of the samples from a profile group.

(Figures 4 and 5). The clustering of Flt3 mutational status with biosignature profiles supports the hypothesis that gene mutations conferring proliferative advantages produce detectable signatures in the mitogenic signaling network of cancer cells (Figures 6 and 7).

Cancer Heterogeneity at the Level of Signaling Response

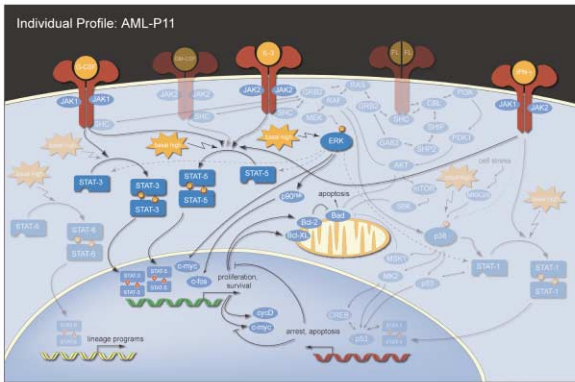
A critical advantage of single cell based biosignatures is that, as shown above, they approximate complex data well enough to allow biologically significant clustering while retaining the underlying flow cytometric data for further examination. We had also examined the original 2D plots of the phospho-protein expression profiles and observed that higher dimensional representations of the data identified subsets of cells with unique signaling features.

Despite being composed of >95% leukemic blasts, the heterogeneity of cytokine responses among AML samples—compared with cell lines or primary cell subsets (Figure 1)—shows the existence of multiple unique cancer subsets based on signaling potential within individual AML patients. Thus, the well-recognized limitation for understanding cancer microheterogeneity might

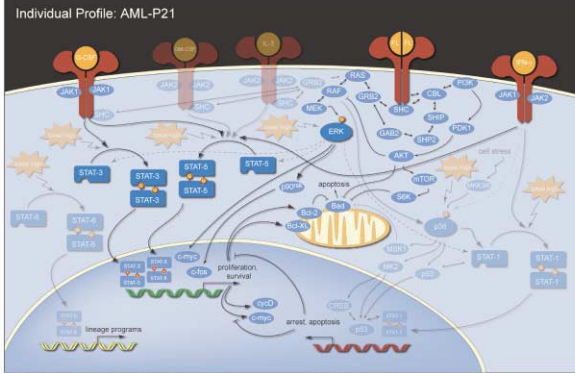
be overcome using multiparameter approaches that distinguish cancer cell subset responses to input stimuli. For instance, although Stat3 and Stat5 are both thought to be constitutively active in leukemias and share many structural similarities, in SC-P2, the Flt3-correlated potentiation of the GM-CSF response only occurred with Stat5 (data not shown, see Supplemental Figure S2); Stat3 showed no response to GM-CSF in any of the tested AML patient samples (Figures 2 and 5). In contrast, in a given cell in SC-P2, the phosphorylation of both Stat5 and Stat3 generally occurred simultaneously following G-CSF stimulation (Figure 5). Interestingly, multiple cancer subpopulations could be observed at the level of the signaling response. For example, AML-P13 and AML-P20 each had a subpopulation of cells that were only p-Stat5 positive in response to G-CSF. However, AML-P11 contained a subpopulation of cells that were p-Stat3 positive in the basal state but unresponsive to the environmental cues applied in these experiments. Whether these subset differences represent simply nonresponsive cells, cancer “stem” cells (Reya et al., 2001), or other stages of clonal evolution within the cancer remains to be determined.

The linkage observed between dual responses and

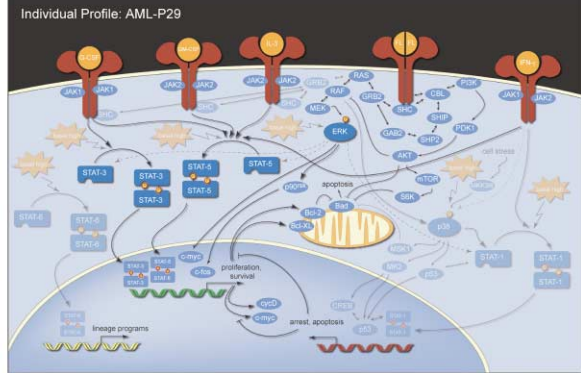
A



B



C



Signaling profile summaries for individual AML patients profiled as SC-P2. Each had detectable Flt3-ITD and resisted course 1 chemotherapy.

Figure 7. Three AML Patients Profiled as SC-P2 Showed Similarities and Differences in Potentiated Signaling Mechanisms
Pathway maps summarizing the signaling phenotype of individual patient samples are shown for three profiled as SC-P2, as per Figure 6. Differences and similarities are highlighted in the text.

Flt3 status suggests strongly that Flt3 mutation can, in significant subset(s) of cells as observed in two-dimensional flow cytometry, lead to unexpected coactivation of important phospho-protein transcription factors. Does this represent a requirement during selective pressure that these cells maintain a low basal state of phosphorylation and then respond to appropriate stimuli for continued cell division? Do the basal high states, combined with nonresponsiveness to cytokine induction, of the SC-NP cancer cells represent a different “solution” that allows for the maintenance of cell division of the cancer? These two cancer escape strategies (distinguished by their network profiles) are differentially responsive to chemotherapeutic induction—and might allow us to use this information to design therapies to attack the aggressive cancer types based on the signaling profile that they present. Extraction of additional high-dimensional information could be applied to further refine our understanding of systems such as those presented here, especially when additional phospho-proteins or other single cell events are measured simultaneously (Krutzik et al., 2004; Krutzik and Nolan, 2003). This could provide the additional information required to understand whether these signaling systems are directly linked to apoptotic responses of proteins such as Bcl-2 and p53 (J.M.I., B.T.G., and G.P.N., unpublished data).

Summary

This study of signaling mechanisms in primary cancer samples indicates that an activated phospho-proteome

can be informative of cancer pathology. The finding that potentiated cytokine responses of these cancers can be combined with information on basal phosphorylation states and clustered to create a classification with clinical relevance helps explain mechanism of signaling functions and might inform the design of mechanism-based cancer therapies. In a broader context, the approach allows a distinction of cell types based on signaling profiles in the absence of other specific knowledge about the differentiation state or pathology of the cell. In this regard, we have observed examples of potentiated signaling in HIV-1 infection (J. Fortin and G.P.N., unpublished data) and in autoimmune systemic lupus erythematosus (P. Krutzik, M. Hale, and G.P.N., unpublished data). While other approaches for measuring multiple events exist, they are usually carried out on “averaged” cell populations (gene chips or high throughput proteomics), whereas multiparameter flow cytometry measures the immediate response of signaling networks at the level of individual cells in complex populations. Measuring the resting state of signaling proteins, and how such proteins align in signaling networks to single or multiple inputs, in correlated datasets at the single cell level therefore provides a fuller understanding of how cells process information in normal and diseased states.

Experimental Procedures

Patients and Preparation of AML Blasts

The study was approved by the local Ethics Committee and samples collected after informed consent. Samples were selected from a

large group of consecutive patients with de novo AML and high peripheral blood blast counts (Bruserud et al., 2003). These patients were admitted to the hospital from April 1999 to August 2003, the median age was 60, and ages ranged from 29 to 84. As these patients were selected for high blast counts, enriched AML cell populations containing >95% cancer cells were prepared using a simple density gradient separation of peripheral blood samples (Ficoll-Hypaque; NyCoMed, Oslo, Norway; specific density 1.077) before safe, standardized cryopreservation according to previously developed techniques (Bruserud et al., 2000). These patients represent the latter portion of a group studied previously for Flt3 signaling and mutation in AML (Bruserud et al., 2003). The acute myeloid leukemia cell line HL-60 and the monocytoid lymphoma cell line U-937 were from American Type Culture Collection (www.atcc.org) and cultured in RPMI medium (Invitrogen, Carlsbad, California) + 10% Fetal Calf Serum (HyClone, South Logan, Utah).

Stimulation of AML Blasts

Peripheral blood containing >95% AML blasts was thawed into 5 ml Stem Span H3000 defined, serum-free medium (Stem Cell Technologies, Vancouver, BC, Canada), counted, pelleted, and resuspended at 2×10^6 cells per ml. Six FACS tubes (Falcon 2052, BD-Biosciences, San Jose, California) were then filled with 2 ml of each leukemia sample and allowed to rest at 37°C for 2 hr. AML blasts were resuspended gently to prevent aggregation and allowed to rest at 37°C for another 45 min. At this time, vehicle (deficient RPMI medium, Invitrogen) or 40 μ l of stimulus was added to each tube to a final concentration of 20 ng/ml. Stimuli included human recombinant Flt3 ligand (FL), GM-CSF, G-CSF, IL-3, and IFN γ (all cytokines from Peprotech, Inc., Rocky Hill, New Jersey). Samples were returned to the 37°C incubator for 15 min to allow signal transduction and phosphorylation, after which 100 μ l of 32% para-formaldehyde (PFA, Electron Microscopy Services Fort Washington, Pennsylvania) was added to each 2 ml tube of cells to a final concentration of 1.6%. Cells were fixed for 15 min at room temperature, pelleted, then permeabilized by resuspension in 2 ml ice cold methanol for 10 min, and stored at 4°C until being stained for flow cytometry.

Intracellular Phospho-Specific Flow Cytometry

PFA fixed, methanol permeabilized AML blasts were rehydrated by adding 2 ml phosphate-buffered saline (PBS), gentle resuspension, and then centrifugation. The cell pellet was washed once with 2 ml PBS, resuspended in 150 μ l PBS + 0.1% BSA (Sigma, St. Louis, Missouri), and split evenly into three new FACS tubes. Fifty microliters of an antibody mix containing 0.065 μ g primary conjugated phospho-specific antibody per sample was added to each tube of AML blasts and staining proceeded for 20 min at room temperature. Alexa (Ax) dye (Molecular Probes, Eugene, Oregon) conjugated antibodies (all from BD-Pharmingen, San Diego, California) included antibodies against phospho-Stat3(Y705)-Ax488, phospho-Stat5(Y694)-Ax647, phospho-Stat6(Y641)-Ax488, phospho-Stat1(Y701)-Ax647, phospho-p38(T180/Y182)-Ax488, and phospho-Erk1/2(T202/Y204)-Ax647 and were applied in pairs (Stat5/Stat3, Stat1/Stat6, and Erk/p38) for subsequent detection of Ax488 and Ax647 on FL-1 and FL-4, respectively. Approximately 30,000 ungated events were collected for each sample on a benchtop FACSCalibur dual-laser cytometer (Becton Dickinson, Franklin Lakes, New Jersey).

Statistical Analysis

Changes in phosphorylation of STAT and Ras-MAPK proteins following cytokine stimulation were approximated by calculating the log₂ ratio of median fluorescence intensity (MFI) of stimulated versus unstimulated cell populations. Differences in basal phosphorylation were compared by calculating the log₂ ratio of each sample's MFI divided by the minimum among cancers. To determine the statistical significance of observed versus expected distributions, we used a χ^2 test (Figure 3B), and to determine the significance of the difference in mean of two populations, we used a student's t test ($\alpha = 0.05$, Figure 4). Standard t tests were used to validate existing hypotheses (Kiyoi et al., 2002; Mizuki et al., 2003).

Derivation of Signaling Pathway Maps

Pathways considered important to the signaling profiles of SC-NP and SC-P2 were identified and highlighted in a model of the probed

network. For an initial appraisal, the following rules were used. Basal nodes were considered "basal high" when more than half the patients in a signaling cluster had signaling above the median for cancers. Similarly, the responsiveness of a node state to an environmental cue was highlighted when more than half of the patient's node states in a profile group were above the median for cancers. Other node states were dimmed. Upon examination, the Stat1 response to IFN γ was dimmed for both SC-NP and SC-P2, as there was an attenuation of this signaling response, relative to donor PBL controls, in both of the main signaling groups. The basal state of p38 and Stat1 were high in SC-NP, but were not observed above the median frequently enough to highlight their activity. Signaling pathway maps were drawn based on multiple sources (McCubrey et al., 2000; Rane and Reddy, 2002; Shuai and Liu, 2003; Stirewalt and Radich, 2003).

Acknowledgments

We thank R. Tibshirani for insights on statistical approaches, O. Vintermyr and A. Molven for making available c-kit and N-ras mutational analysis, A. Eliassen for assistance on Flt3 mutational analysis, N. Ånensen for many useful discussions, R. Smith, R. Wolkowicz, R. Ihrle, and P. Yam for review of this manuscript, and K. Vang for administrative assistance. This work was supported by National Heart, Lung and Blood Proteomics Center Contract N01-HV-281831. O.D.P. is supported as a Bristol-Meyers Squibb Irvington-Institute Fellow and by the Dana Farber Foundation. We gratefully acknowledge the support of BD Biosciences-Pharmingen, and the Baxter Foundation. B.T.G. was supported by the Norwegian Research Council Functional Genomics Program (FUGE) grant number 151859 and the Norwegian Cancer Society (DNK). R.H. and Ø.B. were supported by Helse Vest HF research grants. P.O.K. was supported by a Howard Hughes Medical Institute Predoctoral Fellowship. J.M.I. was supported by the James H. Clark Stanford Graduate Fellowship and the J.G. Lieberman Fellowship.

Received: January 10, 2004

Revised: May 28, 2004

Accepted: May 28, 2004

Published: July 22, 2004

References

- Benekli, M., Xia, Z., Donohue, K.A., Ford, L.A., Pixley, L.A., Baer, M.R., Baumann, H., and Wetzler, M. (2002). Constitutive activity of signal transducer and activator of transcription 3 protein in acute myeloid leukemia blasts is associated with short disease-free survival. *Blood* 99, 252–257.
- Benekli, M., Baer, M.R., Baumann, H., and Wetzler, M. (2003). Signal transducer and activator of transcription proteins in leukemias. *Blood* 101, 2940–2954.
- Birkenkamp, K.U., Geugien, M., Lemmink, H.H., Kruijer, W., and Vellenga, E. (2001). Regulation of constitutive STAT5 phosphorylation in acute myeloid leukemia blasts. *Leukemia* 15, 1923–1931.
- Bowman, T., Garcia, R., Turkson, J., and Jove, R. (2000). STATs in oncogenesis. *Oncogene* 19, 2474–2488.
- Bruserud, O., Gjertsen, B.T., and von Volkman, H.L. (2000). In vitro culture of human acute myelogenous leukemia (AML) cells in serum-free media: studies of native AML blasts and AML cell lines. *J. Hematother. Stem Cell Res.* 9, 923–932.
- Bruserud, O., Hovland, R., Wergeland, L., Huang, T.S., and Gjertsen, B.T. (2003). Flt3-mediated signaling in human acute myelogenous leukemia (AML) blasts: a functional characterization of Flt3-ligand effects in AML cell populations with and without genetic Flt3 abnormalities. *Haematologica* 88, 416–428.
- Buettner, R., Mora, L.B., and Jove, R. (2002). Activated STAT signaling in human tumors provides novel molecular targets for therapeutic intervention. *Clin. Cancer Res.* 8, 945–954.
- Calo, V., Migliavacca, M., Bazan, V., Macaluso, M., Buscemi, M., Gebbia, N., and Russo, A. (2003). STAT proteins: from normal control of cellular events to tumorigenesis. *J. Cell. Physiol.* 197, 157–168.
- Coffer, P.J., Koenderman, L., and de Groot, R.P. (2000). The role of

- STATs in myeloid differentiation and leukemia. *Oncogene* 19, 2511–2522.
- Gilliland, D.G., and Griffin, J.D. (2002). The roles of FLT3 in hematopoiesis and leukemia. *Blood* 100, 1532–1542.
- Hanahan, D., and Weinberg, R.A. (2000). The hallmarks of cancer. *Cell* 100, 57–70.
- Hayakawa, F., Towatari, M., Kiyoi, H., Tanimoto, M., Kitamura, T., Saito, H., and Naoe, T. (2000). Tandem-duplicated Flt3 constitutively activates STAT5 and MAP kinase and introduces autonomous cell growth in IL-3-dependent cell lines. *Oncogene* 19, 624–631.
- Kiyoi, H., Ohno, R., Ueda, R., Saito, H., and Naoe, T. (2002). Mechanism of constitutive activation of FLT3 with internal tandem duplication in the juxtamembrane domain. *Oncogene* 21, 2555–2563.
- Kottaridis, P.D., Gale, R.E., Frew, M.E., Harrison, G., Langabeer, S.E., Belton, A.A., Walker, H., Wheatley, K., Bowen, D.T., Burnett, A.K., et al. (2001). The presence of a FLT3 internal tandem duplication in patients with acute myeloid leukemia (AML) adds important prognostic information to cytogenetic risk group and response to the first cycle of chemotherapy: analysis of 854 patients from the United Kingdom Medical Research Council AML 10 and 12 trials. *Blood* 98, 1752–1759.
- Krutzik, P.O., and Nolan, G.P. (2003). Intracellular phospho-protein staining techniques for flow cytometry: Monitoring single cell signaling events. *Cytometry* 55A, 61–70.
- Krutzik, P.O., Irish, J.M., Nolan, G.P., and Perez, O.D. (2004). Analysis of protein phosphorylation and cellular signaling events by flow cytometry: techniques and clinical applications. *Clin. Immunol.* 110, 206–221.
- Lowenberg, B., Downing, J.R., and Burnett, A. (1999). Acute myeloid leukemia. *N. Engl. J. Med.* 341, 1051–1062.
- McCubrey, J.A., May, W.S., Duronio, V., and Mufson, A. (2000). Serine/threonine phosphorylation in cytokine signal transduction. *Leukemia* 14, 9–21.
- Mizuki, M., Fenski, R., Halfter, H., Matsumura, I., Schmidt, R., Muller, C., Gruning, W., Kratz-Albers, K., Serve, S., Steur, C., et al. (2000). Flt3 mutations from patients with acute myeloid leukemia induce transformation of 32D cells mediated by the Ras and STAT5 pathways. *Blood* 96, 3907–3914.
- Mizuki, M., Schwable, J., Steur, C., Choudhary, C., Agrawal, S., Sargin, B., Steffen, B., Matsumura, I., Kanakura, Y., Bohmer, F.D., et al. (2003). Suppression of myeloid transcription factors and induction of STAT response genes by AML-specific Flt3 mutations. *Blood* 101, 3164–3173.
- Namikawa, R., Muench, M.O., Firpo, M.T., Humeau, L., Xu, Y., Menon, S., and Roncarolo, M.G. (1999). Administration of Flk2/Flt3 ligand induces expansion of human high-proliferative potential colony-forming cells in the SCID-hu mouse. *Exp. Hematol.* 27, 1029–1037.
- Nieborowska-Skorska, M., Wasik, M.A., Slupianek, A., Salomoni, P., Kitamura, T., Calabretta, B., and Skorski, T. (1999). Signal transducer and activator of transcription (STAT)5 activation by BCR/ABL is dependent on intact Src homology (SH)3 and SH2 domains of BCR/ABL and is required for leukemogenesis. *J. Exp. Med.* 189, 1229–1242.
- Pallis, M., Seedhouse, C., Grundy, M., and Russell, N. (2003). Flow cytometric measurement of phosphorylated STAT5 in AML: lack of specific association with FLT3 internal tandem duplications. *Leuk. Res.* 27, 803–805.
- Perez, O.D., and Nolan, G.P. (2002). Simultaneous measurement of multiple active kinase states using polychromatic flow cytometry. *Nat. Biotechnol.* 20, 155–162.
- Platanias, L.C. (2003). Map kinase signaling pathways and hematologic malignancies. *Blood* 101, 4667–4679.
- Rane, S.G., and Reddy, E.P. (2002). JAKs, STATs and Src kinases in hematopoiesis. *Oncogene* 21, 3334–3358.
- Reya, T., Morrison, S.J., Clarke, M.F., and Weissman, I.L. (2001). Stem cells, cancer, and cancer stem cells. *Nature* 414, 105–111.
- Shuai, K., and Liu, B. (2003). Regulation of JAK-STAT signalling in the immune system. *Nat. Rev. Immunol.* 3, 900–911.
- Smithgall, T.E., Briggs, S.D., Schreiner, S., Lerner, E.C., Cheng, H., and Wilson, M.B. (2000). Control of myeloid differentiation and survival by Stats. *Oncogene* 19, 2612–2618.
- Spiekermann, K., Pau, M., Schwab, R., Schmieja, K., Franzrahe, S., and Hiddemann, W. (2002). Constitutive activation of STAT3 and STAT5 is induced by leukemic fusion proteins with protein tyrosine kinase activity and is sufficient for transformation of hematopoietic precursor cells. *Exp. Hematol.* 30, 262–271.
- Stirewalt, D.L., and Radich, J.P. (2003). The role of FLT3 in haematopoietic malignancies. *Nat. Rev. Cancer* 3, 650–665.
- Thiede, C., Steudel, C., Mohr, B., Schaich, M., Schakel, U., Platzbecker, U., Wermke, M., Bornhauser, M., Ritter, M., Neubauer, A., et al. (2002). Analysis of FLT3-activating mutations in 979 patients with acute myelogenous leukemia: association with FAB subtypes and identification of subgroups with poor prognosis. *Blood* 99, 4326–4335.
- Tilstone, C. (2003). DNA microarrays: vital statistics. *Nature* 424, 610–612.
- Turkson, J., and Jove, R. (2000). STAT proteins: novel molecular targets for cancer drug discovery. *Oncogene* 19, 6613–6626.
- Wheatley, K., Burnett, A.K., Goldstone, A.H., Gray, R.G., Hann, I.M., Harrison, C.J., Rees, J.K., Stevens, R.F., and Walker, H. (1999). A simple, robust, validated and highly predictive index for the determination of risk-directed therapy in acute myeloid leukaemia derived from the MRC AML 10 trial. United Kingdom Medical Research Council's Adult and Childhood Leukaemia Working Parties. *Br. J. Haematol.* 107, 69–79.
- Xia, Z., Baer, M.R., Block, A.W., Baumann, H., and Wetzler, M. (1998). Expression of signal transducers and activators of transcription proteins in acute myeloid leukemia blasts. *Cancer Res.* 58, 3173–3180.